Challenges and Prospects of Coulomb Spacecraft Formation Control

Hanspeter Schaub, Gordon G. Parker and Lyon B. King

Challenges and Prospects of Coulomb Spacecraft Formation Control

Hanspeter Schaub[*] **Gordon G. Parker**[†] **and Lyon B. King**[‡]

Abstract

Spacecraft formation flying using Coulomb forces is a relatively new technology for spacecraft control, and may have application for a wide variety of mission objectives including attitude control, collision avoidance, and orbit perturbation correction. Coulomb-controlled formations appear ideally suited for close formation-flying in high Earth orbits to perform wide field of view imaging missions using separated spacecraft interferometry. This paper discusses the challenges and prospects of developing spacecraft formations utilizing Coulomb forces. Formation flying on the order of tens of meters is very difficult using conventional ion propulsion methods, because the exhaust plumes will quickly interfere with the delicate on-board sensors. The Coulomb forces would allow the relative motion of satellites to be controlled without such contaminations. Since the rise time of the spacecraft charging is on the order of milli-seconds, very high bandwidth control is feasible. Further, the fuel efficiency of the control makes very long duration missions possible. Non-Keplerian steady-state orbits are discussed which could be used to generate in-plane or three-dimensional static spacecraft formations. The currently examined static solutions are unstable and require the development of a control strategy. Further, the behavior of a two-satellite Coulomb formation with constant equal or opposite charges is discussed at GEO. A nonlinear, orbit elements based feedback law is then introduced to control the relative motion within a two-satellite formation by stabilizing the orbit element differences about desired values. Global stability is analytically shown and illustrated through a numerical example. Asymptotic stability is proven for a semi-major axis only control about a circular orbit. The lack of general asymptotic stability with inter-spacecraft Coulomb forces is discussed.

Introduction

The SCATHA satellite[1] was launched in January, 1979 with the goal of measuring the build-up and breakdown of electrostatic charge on various spacecraft components, and to characterize the natural environment at Geostationary Orbits (GEO) altitudes. Throughout its mission, the satellite potential was monitored with respect to the space plasma potential. During passive operation, the

---

[*]Assistant Professor, Virginia Tech, Blacksburg, VA 24061.

[†]Associate Professor, Mechanical Engineering Department, Michigan Technological University, Houghton, MI 49931.

[‡]Assistant Professor, Mechanical Engineering Department, Michigan Technological University, Houghton, MI 49931.

spacecraft potential varied from near ground to many kilovolts negative, a common occurrence for High Earth Orbit (HEO) satellites. These variations are directly related to the current solar activity level. An isolated passive body immersed in plasma will attain a negative charge due to a higher electron mobility, as compared to the mobility of heavier ions. For hot plasma, such as is found at HEO or GEO, this negative charge is substantial. One goal of the SCATHA mission was to test the validity of actively controlling the spacecraft potential by emitting charge through an electron beam. To this end, an electron gun was used to transfer charge from SCATHA to the space plasma at various current and voltage levels up to 13 mA and 3 kV. The controllability of spacecraft charge will not depend strongly on local plasma parameters. While the density and temperature will change dependent upon solar cycles, the ability to charge the craft to a known voltage is dependent upon the on-board emission system. Thus, a 3 keV e-beam would be sufficient to charge SCATHA to 3 keV during solar max or solar min.

Due to the plasma environment, spacecraft routinely charge to negative voltages. However, a very important result, as reported by Gussenhoven,[1] et al., was that, "*the electron beam can achieve large, steady-state changes in the vehicle potential and the returning ambient plasma.*" In fact, they found that when a 3 kV electron beam was operated, "*the satellite became positively charged to . . . a value approaching beam energy for 0.10 mA emission current.*" Similarly, Cohen, et al. report that "*spacecraft frame and surfaces on the spacecraft went positive with respect to points 50 meters from the satellite when the gun was operated. Depending upon ejected electron currents and energies, spacecraft frame-to-ambient-plasma potential differences between several volts and 3 kV were generated.*"

For rough calculations, the SCATHA spacecraft can be approximated as a 1.7 meter diameter sphere. If an identical SCATHA spacecraft had been in orbit simultaneously, the satellite electrical potential control demonstrated in the 1979 mission would have been sufficient to actively generate attractive and repulsive forces between the vehicles with magnitudes up to 10 mN over 10 meters, consuming 3 Watts of power. In addition to the SCATHA data, during a separate flight-experiment, the ATS-6 spacecraft demonstrated charging as high as 19 kV.[2–4] Thus, generating hundreds of mN control forces would be possible with a spacecraft 1 meter in diameter.

In 2001 a NASA NIAC study[5] investigated the practicality of modulating spacecraft charge, the charging time constants and propulsion system sizing.[6] Further, this study researched equilibrium points of such Coulomb satellite formations, their local stability, as well as the charge requirements for a variety of geostationary orbit formations. Their conclusion provided some exciting results for formation flying control. It was found that the spacecraft charging is nearly propellantless. It is possible to achieve specific impulses values ranging from 10^7 seconds to values as large as 10^{13} seconds with time constants less than 100 milliseconds consuming under 1 Watt of power. Traditionally, to change a spacecraft orbit, some type of thrusting is required. Due to the conservation of linear momentum, by expelling a small mass at a high velocity, the relatively heavy spacecraft is made to move at a small velocity in the opposite direction. To correct the relative orbit between satellites, the satellites will have to expel fuel to push themselves through space. Small relative orbit adjustments are routinely required of formation flying control systems to correct for external perturbations. Depending on how near-natural (i.e., control-free) the desired relative orbit is, and depending on the relative position tolerance requirements, such corrective thrusts can be required very often. In fact, the life time of a formation flying mission is often limited by how much fuel can be carried on board to perform such relative orbit corrections. However, using electrostatic attractions between spacecraft (i.e., Coulomb forces), it is possible to directly control the relative motion of the satellites, without influencing the overall orbital motion of the entire formation. Since

the Coulomb forces are internal forces, they will have zero effect on the formation center of mass motion. The relative motion is controlled through the electric fields generated by the spacecraft. Since it requires a minuscule amount of fuel mass to generate these electric fields (mass required to operate the electron or ion gun), it is possible to achieve the high specific impulse values to control relative motion. Further, conventional propulsive devices rely on discrete impulse bits to control fine positioning. Factors limiting the positioning accuracy within a swarm include repeatability of impulse bits, random off-axis thrust components, and resolution of impulse control. The Coulomb concept allows for continuous, fine-resolution maneuverability, which will greatly improve formation tolerances due to the high bandwidth at which the Coulomb forces can be continuously varied.

The generation of electrostatic Coulomb forces is only possible in the higher Earth altitudes because of the plasma space environment. At lower altitudes, the Debye shielding effect screens electric fields over short distances.[6] Further, since the electric field decreases with the radial separation of the spacecraft, the relative orbit size is limited to 10–100 meters in size to avoid excessive electric charges of the craft. While traditional spacecraft formations typically investigate relative orbits of the size of 1–100 kilometers, the application of Coulomb forces enables an entirely different class of spacecraft formation. Close formation flying of the order of a few dozen meters is a very difficult and dangerous operation using conventional ion thrusters. Operating in such close quarters, the thruster exhaust plumes are likely to damage the delicate on-board sensing equipment of the spacecraft. Micro-thrusters currently envisioned for swarm formation-flying emit propellant such as Teflon or cesium. Many science missions, benefiting from formation flying concepts, will carry sensitive diagnostic equipment. In close proximity operations, propellant exhaust from micro-thrusters has a high likelihood of adversely impinging upon neighboring craft, and hence disabling diagnostics.

Reconciling the capabilities and limitations of Coulomb control with the benefits of Separated Spacecraft Interferometry (SSI), a class of interesting missions that would be uniquely enabled with the proposed concept becomes evident: large field-of-view planetary imaging with unprecedented resolution. Consider, for instance, space-based Earth imaging. Using classical monolithic optics, the minimum achievable image resolution is inversely related to the size of the collecting optic. Since the size of a single space-based collecting optic is limited by launch vehicle fairing constraints, Earth-imaging spacecraft with meter-level surface resolution have been limited to altitudes below a few hundred kilometers. In such low orbits, the spacecraft field-of-view is limited to a small portion of the Earth's surface and the target dwell time is short due to the fast orbit. Using an SSI system, it would be possible to provide visible Earth imaging from GEO with meter-level surface resolution. Such a distributed space system would have a field-of-view of nearly an entire hemisphere with an unlimited target dwell time. The benefits to the scientific community would be truly global monitoring capabilities of weather systems, ocean currents, etc.

The Coulomb concept is uniquely suited to such large field-of-view imaging systems. It can be shown that meter-level surface resolution from GEO with realistically sized individual spacecraft operating in an SSI requires formation spacing on the order of tens of meters.,[5,7] Although a structurally connected set of distributed apertures could provide the required imaging baselines, the use of SSI enables dynamic reconfiguring of the imaging formation in order to optimize parameters whose priorities may change during the mission. The requirements for high-orbit imaging of other solar system planets are similar. For such missions, electric micro-thrusters are not feasible. Even if electric thrusters could provide the required formation position tolerances, the caustic propellant efflux arising from continuous thruster firings in close proximity would produce intolerable contamination environments. Furthermore, the potential for inter-vehicle collision would be unsettling.

This paper discusses various fundamental aspects of achieving Coulomb spacecraft formations (CSF). The first section presents the basic Coulomb force modeling in an Earth orbit environment and discusses at what altitudes these forces become useful for spacecraft control. The second section reviews some static equilibrium configurations that have been found and discusses the controllability thereof. The last chapter discusses the basic relative motion of a two-satellite system which is using Coulomb forces to establish a bounded relative motion and attempts to drive the orbit element differences to desired values.

Generating Coulomb Forces

Physics of Producing Coulomb Forces in Space

Let us examine in detail how electric potential fields are generated about a spacecraft in orbit. Consider the space plasma environment to consist of negatively charged electrons and positively charged ions. The smaller plasma electrons are generally much faster than the heavy ions. Thus, in a given unit of time more plasma electrons than ions could reach the spacecraft, which would result in an unacceptable net current (charging rate) to the vehicle. However, assuming that the spacecraft has no initial potential, then these electrons will accumulate and cause the vehicle potential to creep to some negative value. This generates a negative electric field around the vehicle, causing more electrons to be repelled and more positively charged ions to be attracted. This in effect reverses the previous tendency to have more electrons hit the craft than ions. Once an equilibrium is established, the spacecraft negative electric field steady-state strength will be such that an equal amount of faster electrons and slower ions will hit the craft and the resulting the net current to the craft is zero. Depending upon the local plasma density of electrons/ions and the local temperature (energy) of electrons/ions, the spacecraft will respond with different distributions of voltages to balance the currents from space. Thus, without applying any control, the spacecraft will naturally assume some negative charge in this space plasma environment. References 5 and 6 investigated the resulting force between two spacecraft due to this natural charging and found it to be surprisingly large. During the worst case plasma conditions at GEO (resulting in the worst spacecraft charging), the net inter-spacecraft force could grow as large as 1 mN with a separation distance of 10 meters. The term "worst case plasma conditions at GEO" refers to those plasma conditions during which the most severe passive spacecraft charging can be expected. These conditions have commonly been called "worst case" since they are used to predict possible disruptive charging to conventional spacecraft. Thus, these conditions imply that, in the absence of a charge emission system, the highest absolute and differential charging can be expected, usually to some large negative potential due to high-energy electrons. This does not necessarily mean that the largest power expenditures would be required to control the vehicle charge. For instance, if it is desired to drive the vehicle charge negative, less power is required because the "worst case" electrons already drive the system in that direction. These conditions do not affect the range of spacecraft forces achievable.

An isolated spacecraft will assume an equilibrium potential (voltage) such that the net environmental current due to plasma and photoelectron emission is zero. It is possible to change this passive equilibrium potential by actively emitting an electrical charge from the spacecraft as illustrated in Figure 1. For example, if it is desired to drive the spacecraft potential lower than equilibrium (more negative), the emission of positive ions from the vehicle will cause a net surplus of on-board electrons and a lowering of the potential. Emission of electrons has the opposite effect. In order to emit such a current, the charges must be ejected from the vehicle with sufficient kinetic energy to escape the spacecraft potential well. Thus, if the vehicle is at a (negative) potential $-V_{SC}$, then ions must
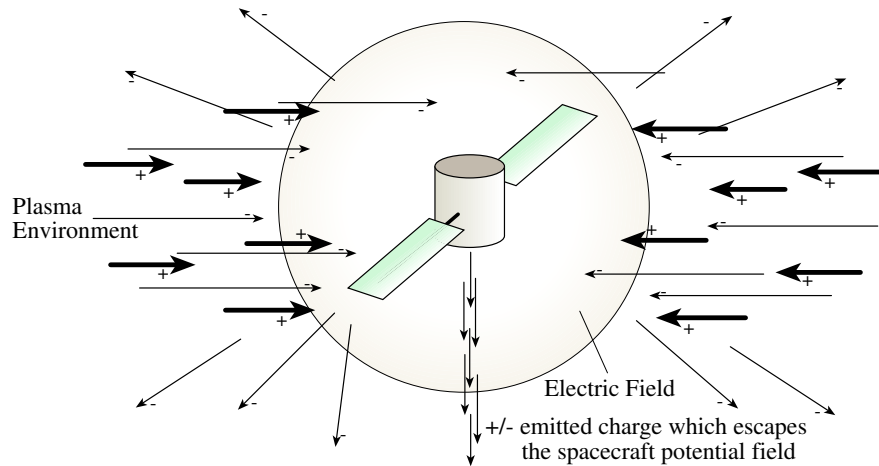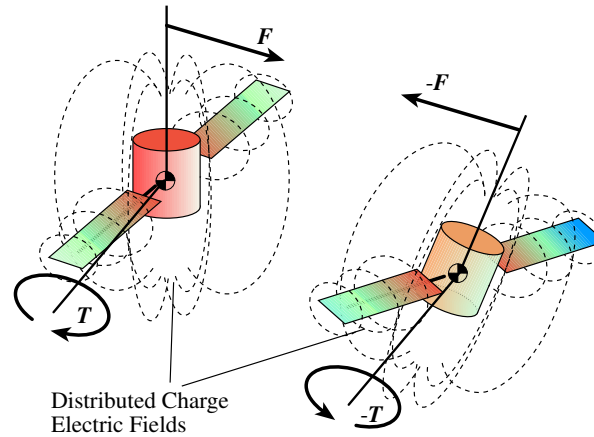
Figure 1: Simple Illustration of the Spacecraft Charging in a Plasma Environment

be emitted from a source operating at a power supply voltage, V_{PS}, greater than $|-V_{SC}|$. Note that to maintain a non-equilibrium spacecraft charge a continuous stream of electrical charge must be emitted from the spacecraft. If this outflow of charge is stopped, then the natural space plasma environment will rebalance the spacecraft charge to the equilibrium levels.

Differential spacecraft charging occurs when portions of the satellite assume different potentials (voltages). The exposed vehicle surfaces will interact with the ambient plasma differently depending on the material composition of the surface, whether the surface is in sunlight or shadow, and the flux of plasma particles to this surface. Another crucial source of differential charging are solar panels. These devices will inherently generate a voltage differential across their surface which is used to power the craft. If the electrical breakdown threshold is exceeded between two components, electrostatic discharge (ESD) can occur. Such a discharge could result in logic switch failures, or even a complete break-down of the electrical sub-systems. Catastrophic ESD's can occur from potential differences of only a few hundred volts between sensitive components. Thus, great design effort needs to be placed in the elimination of spacecraft differential charging. In particular, increasing the overall negative voltage on the spacecraft could increase the incidence of discharge arcing on the solar arrays, due to large potential differences between the arrays and the spacecraft bus. The NASA Space Environment Effects (SEE) Interactive Spacecraft Charging Handbook[8] provides guidelines to model the plasma environment and spacecraft charging. With the spectre of ESD looming, it seems foolhardy to propose intentional charging of spacecraft to potentials of tens of kV (in the current study, potentials are limited to 40 kV over a 1-m-radius spacecraft, or equivalently a charge of 4 micro-Coulombs). It must be noted that the Coulomb control concept proposes uniform absolute charging of the entire spacecraft. While such absolute charging, by itself, has no risk for the vehicle, current spacecraft are typically not designed to be able to handle such large voltages. A CSF satellite would need to be designed to be able to handle these larger charges and voltages by limiting differential charging across its components.

Besides potentially causing ESD, differential spacecraft charging can also affect the motion of the spacecraft. Figure 2 illustrates two spacecraft with non-uniform electrical charging (shown through different satellite shading). Each charged component of a spacecraft will attract or repel other charged components of the spacecraft. Summing up these forces and torques about the craft mass center, they will naturally cancel each other since they are internal forces of the spacecraft body.

Figure 2: Illustration of Exploiting the Net-Torques due to Non-Uniform Spacecraft Charging to Perform Attitude Maneuvers

Only if the spacecraft is flexible will these distributed charge forces cause motion (in the form of bending and flexing) of a single spacecraft. However, consider the case where a second spacecraft is in close proximity and also contains a distributed charge electric field. Now summing up the attracting and repulsive forces between the two spacecraft components, we find that the distributed charges can result in a net torque being applied to each spacecraft. To conserve the total angular momentum of the system, these torques will be equal in magnitude, but in opposite directions. Thus, if two satellites in a CSF are in close proximity, then the distributed charge electric field *must* be taken into account. The simpler point charge model will still dictate the motion of the craft center of masses, but the distributed charge model will determine the attitude changes of the vehicles. In Reference 6 it was found that the natural distributed charge that would occur during worst case plasma conditions (i.e. causing the worst space craft charging) at GEO could result in torques as large as 0.1 μNm at 10 meter separation distance.

The distributed spacecraft charging phenomena results in two types of scenarios. Either these external torques will need to be compensated for by the satellite attitude control system (reaction wheels, control moment gyroscopes, etc.), or they can be taken advantage of to perform *desired* attitude maneuvers. For example, the spacecraft could be designed to allow for predictable and controlled distributed charging of the craft, which could then be taken advantage of to perform attitude maneuvers. If one vehicle has a conventional momentum based attitude control system, then it would be able to perform an attitude change and reorient a second spacecraft in close proximity at the same time. Naturally, the primary spacecraft's momentum wheels would be working twice as hard here to rotate its own spacecraft and compensate for the external Coulomb-based torque applied by the second spacecraft. An inherent limit of this concept of exploiting distributed spacecraft charging to perform attitude maneuvers is that the spacecraft must be in very close proximity to each other (typically 10-30 meters apart). As the separation distance increases, any distributed charge electric field will begin to resemble that of a simple point charge.

Another type of CSF that merits mention is a dumbbell shaped spacecraft illustrated in Figure 3 where $q_1 = q_2$. Here no ESD is possible since there is no charge gradient across the craft. However, the end mass which is closer to the second craft m_0 will experience a stronger electrical field, and thus a stronger Coulomb force, then the second end mass. This effect is similar to having a gravity gradient stabilize the attitude of a spacecraft. Contrary to the previous attitude maneuver example
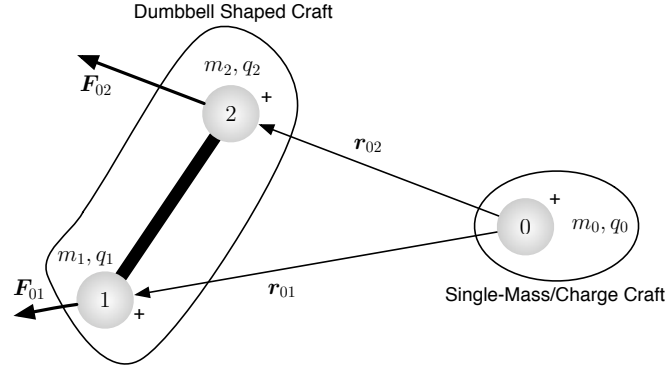
Figure 3: Illustration of Dumbbell-Type Spacecraft Performing Attitude Maneuvers using Coulomb Forces Relative to a Single-Charge Craft

using differential spacecraft charging, note that here no momentum based attitude control system is required. Total momentum, on the other hand, will always be conserved during these Coulomb force based attitude maneuvers, which will require that relative motion and attitude maneuvers are performed in a collaborative manner.

Basic concepts can be used to calculate the power required to maintain the spacecraft at some steady state potential. To maintain the spacecraft at a voltage of $|V_{SC}|$, current must be emitted in the amount of $|I_e| = 4\pi d^2|J_p|$, where J_p is the current density to the vehicle from the local space plasma and d is the vehicle radius, using a power supply having voltage of at least $|V_{PS}| = |V_{SC}|$. Quantitatively, we find that the power P is given by

$$P = |V_{SC}I_e| \tag{1}$$

For a two-spacecraft formation with each vehicle using power P, the total system power is just the sum of the individual powers of each vehicle. Assuming spherical spacecraft and using Gauss Law to relate the surface potential to the encircled point charge, it is possible to relate the Coulomb force (thrust) on a vehicle to the emission current and the required power through

$$F_c = \frac{1}{k_c}e^{-\frac{r_{12}}{\lambda_d}}\frac{d_1 d_2}{r_{12}^2}\frac{P^2}{I_{e_1}I_{e_2}} \tag{2}$$

where d_i and I_{e_i} are the radius and emission current of spacecraft 1 or 2, r_{12} is the vehicle separation, λ_d is the Debye length,[9, 10] and $k_c = 8.99 \cdot 10^9$ Nm²/C² is Coulomb's constant. Assuming $d_1 = d_2 = d_{\text{sc}}$, and $I_{e_1} = I_{e_2} = I_e$, the fuel efficiency of a CSF is[6]

$$I_{sp} = k_c e^{-\frac{r_{12}}{\lambda_d}}\frac{q_{\text{ion}}d_{\text{sc}}^2 P^2}{g_0 m_{\text{ion}}r_{12}^2 I_e^3} \tag{3}$$

Note that this specific impulse estimation only makes sense when two or more spacecraft are present, because the Coulomb force can only influence the relative motion between craft.

While the Coulomb spacecraft formation flying concept envisions ejecting positive ions from the craft, the thrusting phenomena is inherently different from that of a traditional ion thruster. For Coulomb "thrusting," the charge transport of the ions is exploited, wherein an ion thruster is used to transport linear momentum. Coulomb forces of tens to hundreds of micro-Newtons can be generated (at spacecraft separations of tens of meters) with as little as a few milli-Watts of spacecraft power,

producing propulsion system specific impulse values with an expected range of 10^{10}–10^{13} seconds with only 10 Watts of power or less.[6] Hence, the Coulomb control concept is nearly propellantless. Furthermore, the Coulomb control forces can be rapidly dithered over a continuous range on a time scale of milliseconds using spacecraft power much less than 1 Watt. For example, in Reference 5 a 1 meter spacecraft was found to be able to charge to 6 kV in as little as 8 ms using only 200 mW of power. As a comparison, the European FEEP thruster has I_{sp} values between 3,000 and 10,000 seconds with thrust ranging 1-100 μN.[11] The USAF is now working on a micro pulsed plasma thruster (micro-PPT) with thrust from 20-80 μN and power from 2-10 W, with I_{sp} values of a few hundred (maybe 500) seconds.[12]

The Coulomb propulsion concept development requires no inherently new devices or technology. In fact, vehicle charge control such as that proposed in this study has been demonstrated in the 1970s on spacecraft such as SCATHA.[1] The technological revolutionary nature of the CSF concept relies on an innovative integration of existing technologies and simple physical principles to provide an extremely fuel efficient method to control the *relative motion* of close-proximity spacecraft. Since the Coulomb forces are internal forces of the spacecraft formation, note that the *inertial orbital motion* of the formation center of mass is not directly influenced by this control concept. However, considerable challenges remain in how to control such CSFs while considering the natural orbital dynamics. The last section will illustrate some results in controlling simple two-body CSFs.

Computing the Electrostatic Forces

Due to the nature of the plasma fields encountered in Earth orbit, the Coulomb force interaction between separation is limited to regimes where the separation distance is less than the plasma Debye length λ_d. The Coulomb force magnitude between two point charges q_1 and q_2 in such a plasma field is given by

$$|\boldsymbol{F}| = k_c \frac{q_1 q_2}{r_{12}^2} e^{-\frac{r_{12}}{\lambda_d}} \tag{4}$$

The smaller the Debye length is, the shorter the effective range is of a given electrical charge. In Low-Earth Orbit (LEO), this length is of the order of centimeters. Thus, using Coulomb forces at such low altitude orbits is impractical. The analysis of CSFs is limited to High-Earth Orbits (HEO) or Geostationary Orbits (GEO), where the Debye length is much larger and allows for CSF dimensions of several dozens of meters. If orbiting other planets or moons, depending on the local plasma environment, it would be possible to establish CSFs at lower altitudes. At GEO altitudes there is a wealth of plasma-physical data available. In particular, the particle detectors on the ATS[2–4] and SCATHA[1] spacecraft measured the plasma variations from 1969 to 1980 with a temporal resolution of 1 to 10 minutes. Calculations based on this data show that the Debye length at GEO ranges from about 140 meters to greater than 1400 meters. This parameter can vary due to the geomagnetic activities, as well as plasma injection events (i.e., a sudden appearance of dense, relatively high energy plasma at GEO occurring at local midnight).

If N satellites are present in a CSF, then the electric field $\boldsymbol{E}_i$ that satellite i will experience due to the other satellites is given by

$$\boldsymbol{E}_i = k_c \sum_{j=1}^{N} q_j \frac{\boldsymbol{r}_{ji}}{|\boldsymbol{r}_{ji}|^3} e^{-\frac{|\boldsymbol{r}_{ji}|}{\lambda_d}} \tag{5}$$

where $i \neq j$ and $\boldsymbol{r}_{ji} = \boldsymbol{r}_i - \boldsymbol{r}_j$ is the relative position vector. Note that we have not assigned any coordinate frame to this potential field expression. As such, the given expression is valid for both

an inertial and Hill frame specific equations of motion description. Assuming the ith spacecraft has a charge q_i, then the electrostatic Coulomb force $\boldsymbol{F}_i$ is

$$\boldsymbol{F}_i = q_i \boldsymbol{E}_i \tag{6}$$

The external acceleration experienced by the ith spacecraft due to the other spacecraft electrical charges is

$$\boldsymbol{a}_i = \frac{1}{m_i} \boldsymbol{F}_i \tag{7}$$

Assuming a maximum spacecraft charge of 4 μC (about 40 kV for a 1 meter radius vehicle), Figure 4 illustrates the Coulomb force strength for separation distances between 10 and 100 meters. The force magnitudes are shown for both a Debye length of 140 meters (worst case) and 1400 meters. At 10 meter separation, the force magnitude grows as large as 1.3 mN and drops off with increasing separation distances. Note that at 50–60 meter separations, the force magnitude is still around 50 μN. The traditional high-efficiency ion thrusters have thrust levels of about 50 μN.
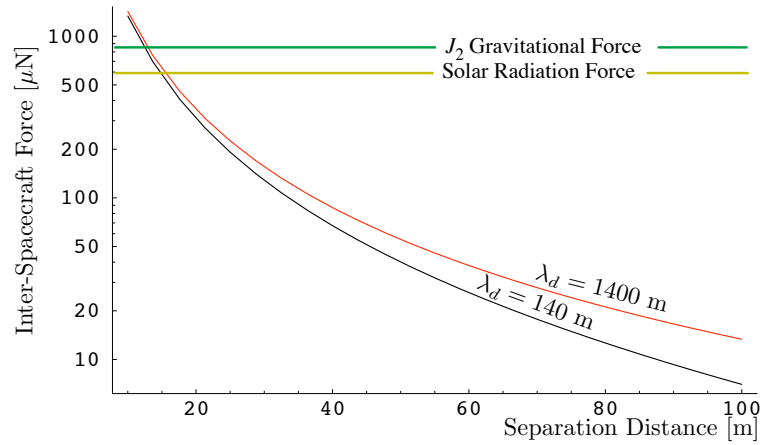
Figure 4: Inter-Spacecraft Coulomb Force Illustration for a 4 μC charge between Two GEO Satellites.

As a comparison, the approximate force magnitude levels of the J_2 gravitational attraction and the solar radiation pressure at GEO are shown as well. Here a spacecraft of 100 kg mass and a radiation surface area of 10 m^2 are assumed. Note that these are the absolute force magnitudes of these two perturbation effects, not the differential force magnitude between the two spacecraft. The latter is mission specific and depends on the relative formation geometry and spacecraft attitudes. However, to illustrate approximate forces needed to compensate for these effects, the differential J_2 force will be at least two orders of magnitude smaller than the absolute force shown, while the differential solar radiation force can conservatively be assumed to be 1 order of magnitude smaller. This illustrates that the Coulomb force magnitudes at GEO are large enough to potentially be able to compensate for these two orbit perturbation effects. Future research will investigate how such formations would be controlled and how the optimal formation geometry would be setup.

Hill's Formulation and Equilibrium Formations

The Hill's equations for N charged spacecraft were derived by Chong et al.[6, 13] and are summarized in this section. The motivation was to examine several specific non-Keplerian formations, and to investigate the possibility of using the Coulomb forces to balance the gravitational forces. Three of these formations will be considered below to illustrate some challenges associated with their closed-loop control. It should be noted that these problems have not yet been solved, but if certain limitations can be overcome, then charged spacecraft control may yield the ability to produce tightly spaced, non-Keplerian formations.

Charged Spacecraft Dynamics

Figure 5 illustrates the notation used in the N charged spacecraft dynamic equations. Specifically, the rotating Local-Vertical-Local-Horizontal (LVLH) frame, sometimes also called the Hill frame, is in a circular orbit about the Earth with constant mean angular rate n. The distance from the center of the Earth to the origin of the orbiting frame, r, is assumed to be much larger than the distance from the center of the orbiting frame to any of the spacecraft, $|\boldsymbol{r}_{0i}|$.
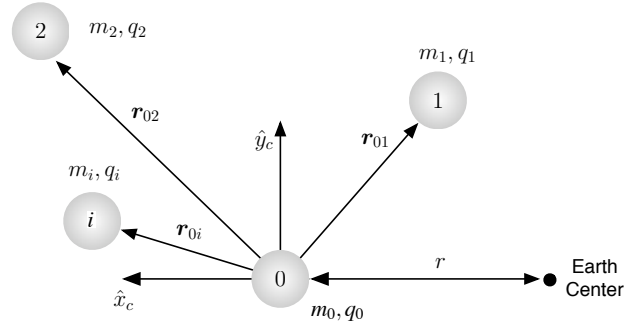
Figure 5: Coordinate Frames and Notation Used for Deriving Hill's Equations for Charged Spacecraft.

Two sets of dynamic equations will be considered, but both are embodied by Eq. 8, where the indices for the equations of motion are always $i = 1, \ldots, N$ and $i \neq j$. The first case, $j_0 = 0$, assumes that the center of the reference frame is coincident with the '0' spacecraft and that it has its own station-keeping propulsion system, and the ability to take on a controlled charge. Therefore, the mass of '0' is not relevant as its motion is prescribed. Furthermore, the origin of the reference frame is not, in general, at the center of mass of the formation. In the second case, there is no '0' spacecraft and consequently $j_0 = 1$ and q_0 is undefined. It may be convenient, though not necessary, to place the origin of the reference frame at the formation's center of mass.

$$\ddot{x}_i - 2n\dot{y}_i - 3n^2 x_i = \frac{k_c}{m_i} \sum_{j=j_0}^{n} \frac{x_i - x_j}{|\boldsymbol{r}_{ji}|^3} q_i q_j \tag{8a}$$

$$\ddot{y}_i + 2n\dot{x}_i = \frac{k_c}{m_i} \sum_{j=j_0}^{n} \frac{y_i - y_j}{|\boldsymbol{r}_{ji}|^3} q_i q_j \tag{8b}$$

$$\ddot{z}_i + n^2 z_i = \frac{k_c}{m_i} \sum_{j=j_0}^{n} \frac{z_i - z_j}{|\boldsymbol{r}_{ji}|^3} q_i q_j \tag{8c}$$

The left side of Eq. 8 are the standard Hill's equations. The right side contains the Coulomb interaction forces between spacecraft where q_i is the charge of the ith satellite. The nonlinear gravitational terms are ignored at this point of the investigation because we are studying a circular chief orbit case with a very small relative orbit radius of less than 100 meters.

In the remainder of this section the results of Chong will be summarized with particular attention towards the goal of controlling the formation using the spacecraft charges. An alternate approach will then be described and its own challenges discussed.

Equilibrium Formations with a Station-Keeping Chief

The first analysis of Eq. 8 was to determine if formations existed, and corresponding constant spacecraft charges, that would maintain a static equilibrium of the spacecraft relative to the moving reference frame. For the case where the '0' spacecraft has its own station-keeping capability, this condition is

$$-3n^2 x_i = \frac{k_c}{m_i} \sum_{j=0}^{n} \frac{x_i - x_j}{|\boldsymbol{r}_{ji}|^3} q_i q_j \tag{9a}$$

$$0 = \frac{k_c}{m_i} \sum_{j=0}^{n} \frac{y_i - y_j}{|\boldsymbol{r}_{ji}|^3} q_i q_j \tag{9b}$$

$$n^2 z_i = \frac{k_c}{m_i} \sum_{j=0}^{n} \frac{z_i - z_j}{|\boldsymbol{r}_{ji}|^3} q_i q_j \tag{9c}$$

Several formations have been found that satisfy Eq. 9. However, they have all been determined to be unstable equilibrium points. Two interesting cases involve three satellites and seven satellites. The three satellite case is helpful as a starting point for examining equilibrium, stability, and control, because formations in the (x_c, y_c) plane reduce the dimensionality of the analysis as the z axis motion is decoupled. The 7 satellite case is interesting since it uses a crystal-like structure to create a 3-D equilibrium formation.
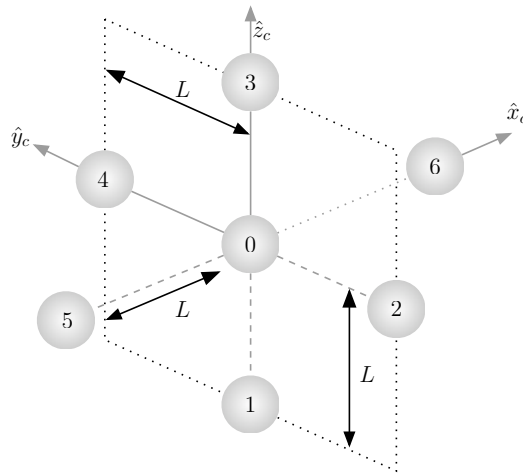
Three Satellite Equilibrium Formation

The right triangular, non-Keplerian formation shown in Fig. 6 satisfies Eq. 9. In fact, this shape constitutes a family of equilibrium formations by rotating the $\boldsymbol{r}_{01}$ and $\boldsymbol{r}_{02}$ equally about the z_c axis. As long as the legs of the triangle do not lie on either x_c or y_c, then constant charges q_0, q_1, and q_2 exist such that the formation will remain fixed. It should be noted that the station-keeping propulsion system of satellite '0' must work continuously to maintain this non-Keplerian formation.

After finding equilibrium formations and assessing stability, Chong proceeded to examine the controllability of the linearized dynamics for small perturbations in satellite position and charge. The three satellite formation was found to be controllable, in the (x_c, y_c) LVLH plane. Presumably, if the linearized system is controllable, then a linear control law could be constructed. The major drawback of this approach is that the radius of convergence could be impractically small. A better, and more global approach, would be to design feedback controllers for the nonlinear Hill's dynamics where stability could be proved using Lyapunov's direct method. Unfortunately, this leads to another type of difficulty for formations of three or more spacecraft.

The nonlinear Hill's equations of Eq. 8 can be rewritten by replacing quadratic charge terms by single inputs. For example the input products $q_0 q_1$, $q_0 q_2$ and $q_1 q_2$ can be considered as simply
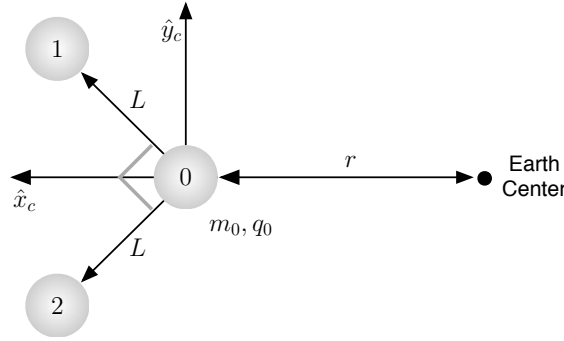
Figure 6: Three Satellite equilibrium Formation where Spacecraft '0' can have a Charge While Maintaining a Circular Orbit using its own Station-Keeping Propulsion System.

Figure 7: Seven Satellite Equilibrium Formation where Spacecraft '0' Can Have a Charge While Maintaining a Circular Orbit Using its Own Station-Keeping Propulsion System.

the combined inputs u_{01}, u_{02} and u_{12}. In this form a standard Lyapunov stable control law can be constructed based on, for example, maintaining the desired lengths of the triangular formation. Unfortunately, not all sets of u_{01}, u_{02} and u_{12} can be realized by the charges q_0, q_1 and q_2. For instance, it is impossible to realize a set of u's where one is negative and the other two are positive, that is, the following relationship must hold.

$$q_0^2 = \frac{u_{01}u_{02}}{u_{12}} \tag{10}$$

Seven Satellite Equilibrium Formation

   Although the planar three satellite formation is convenient for exploring fundamental aspects of Coulomb spacecraft control, it has the limitation that any out-of-plane perturbation will result in unbounded motion. Chong investigated a crystal-like seven satellite formation shown in Fig. 7.

   Again, constant charges can be found that maintain equilibrium. However, the equilibrium is
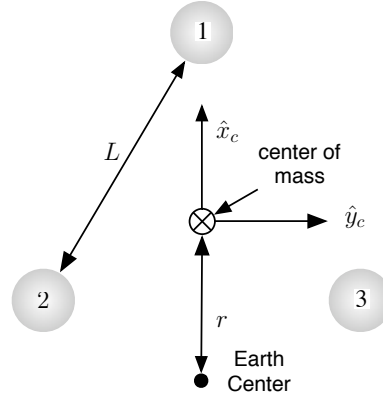
Figure 8: Three Satellite Equilibrium Formation in the Shape of an Equilateral Triangle, where All Spacecraft are Free-Flying using Only Coulomb Forces and No Station Keeping Propulsion Systems.

unstable, and 10 states (out of 36) of the linearized system are uncontrollable. The challenge with crystal-like formations is to find equilibrium conditions where all the states are controllable. The previous development of three-dimensional equilibrium conditions had not taken this into account.

Equilibrium of a Free-Flying Formation

As pointed out in the previous section, the work by Chong focused on equilibrium formations where the '0' spacecraft had its own station keeping propulsion system. Potentially, it would need to exert substantial fuel to maintain the non-Keplerian formation. In this section a new three satellite formation is presented where the reference frame is at the formation center of mass. Although non-Keplerian, the formation requires no traditional station keeping propulsion system to maintain the equilibrium formation.

The equilateral triangle formation, shown in Fig. 8 permits constant equilibrium charges of

$$q_1 = n\sqrt{\frac{2mL^3}{k_c}} \qquad q_2 = q_3 = -n\sqrt{\frac{mL^3}{2k_c}} \tag{11}$$

These are derived from solving the equilibrium equations of Eq. 9 assuming that all spacecraft have equal mass $m_1 = m_2 = m_3 = m$. This is an attractive alternative to Chong's formations, since it is truly a free-flying, non-Keplerian formation. However, it still suffers from the difficulty of closed-loop control due to the quadratic nature of the input. Although this example illustrates the ability to form an equilibrium configuration in a plane, to fully realize the benefits of Coulomb controlled spacecraft, several areas need further exploration. Specifically, the existence of 3D free-flying formations should be ascertained, including the possibility of producing stable equilibrium configurations.

Dynamic Two-Satellite Formation

Static Charge Study

Before developing a Coulomb control law for a dynamic two-satellite formation, let us investigate how the in-plane relative orbit of two satellites will evolve under the influence of static electrical

fields. In particular, relative orbit motion is of interest at GEO altitudes. With the CSF concept, one potential application is to have the fields be used to cause the satellites to repel each other and avoid collisions. However, with the rotational orbital motion of the satellites, this task can become non-trivial.

At GEO altitudes, the orbital path curvature is relatively small compared to those of Low-Earth Orbits (LEO) altitudes. At first glance it might seem that with the relatively tight CSF relative orbits (nominal minimal separation distances of 10–100 meters) and the high GEO altitude that an equal charge on both satellites would cause them to move further apart. This would be true if the formation were operating in space removed from local gravity fields (on a heliocentric orbit, for example), where the only influence on the satellite motions would be the electric attraction/repulsion. However, it was found that even with these short separation distance the orbital motion cannot be ignored.

The following simulations numerically solves for the relative motion between two identical satellites with a mass of $m = 150$ kg. The nonlinear inertial equations of motion solved are

$$\ddot{\boldsymbol{r}}_i + \frac{\mu}{r_i^3}\boldsymbol{r}_i = \boldsymbol{a}_i \tag{12}$$

where the external acceleration $\boldsymbol{a}_i$ is given by Eq. (7). Satellite 1 has an initial semi-major axis a of 42241.09516 km, an eccentricity e of 0, an inclination i of 48º, an ascending node Ω of 20º, an argument of perigee ω of 0º, and an initial mean anomaly M_0 of 20.0º. The period for this GEO orbit is 24 hours. Satellite 2 has the identical orbit elements, initially, except for an initial mean anomaly being $M_0 = 20.0001$ degrees. This puts the two satellites in a classical leader-follower formation with the second satellite being about 70 meters ahead of the first satellite. Note that the complete nonlinear differential equations were solved here, but no non-Keplerian perturbations were included except for the Coulomb force. A constant Debye length of 140 meters is assumed.

Figure 9(a) shows the resulting in-plane motion as seen by a LVLH frame attached to the formation mass center for up to 5 orbit periods. In this coordinate system, x is radially outward and y is along the orbit velocity vector as illustrated in Figure 5. Both satellites have the same small charge of 0.1 μC. Without the orbital dynamics present, this would cause the two satellites to push apart. At first glance it appears like the two satellites immediately begin to pull together, despite both craft having a positive electrical charge. However, closely examining the initial motion does reveal that the two craft first start to separate, as expected. However, because both satellites are pushing off from each other in a leader-follower formation, this causes the lagging satellite 1 to inertially slow down, while the leading satellite 2 is sped up slightly. This results in satellite 1 having a faster orbit period (smaller semi-major axis, as shown in Figure 9(b)) and to pull ahead, while satellite 2 has a slower orbit period (larger semi-major axis) and falls behind. Thus, despite the intention of repulsing both spacecraft with an equal charge, even the diminished orbital dynamics at GEO can cause the opposite effect. Note that this particular motion shown did not recover. With longer simulations the craft quickly separated since their semi-major axes settled down at unequal values, as illustrated in Figure 9(b).

The second simulation has satellite 1 charged to +0.1 μC and satellite 2 charged to -0.1 μC. The simulation results are shown in Figure 10. Here the two craft initially pull together, which in return slows down the lagging craft and speeds up the leading craft. Since the semi-major axis of each satellite settle at unequal values as shown in Figure 10(b), this formation too will grow unbounded. These simulations illustrate that even at GEO and with the small separation distances considered for CSFs, the classical orbit rendezvous dynamics must be taken into account.
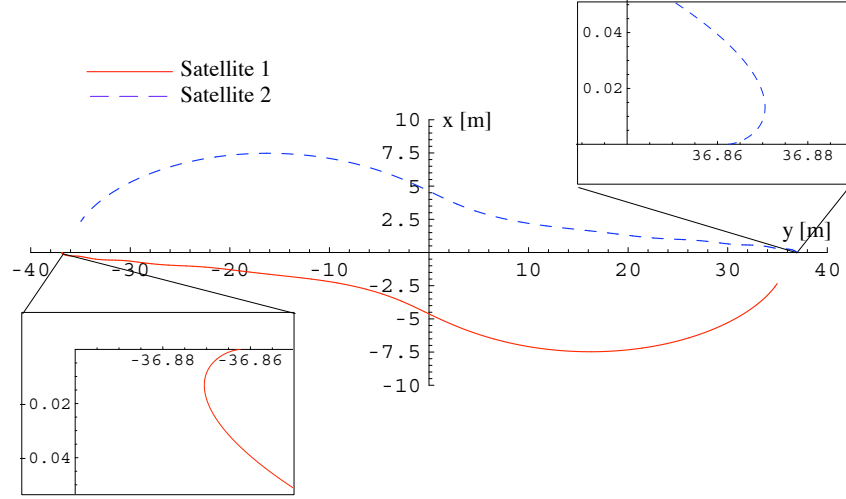
(a) Relative Orbit Motion As Seen by Mean LVLH Frame
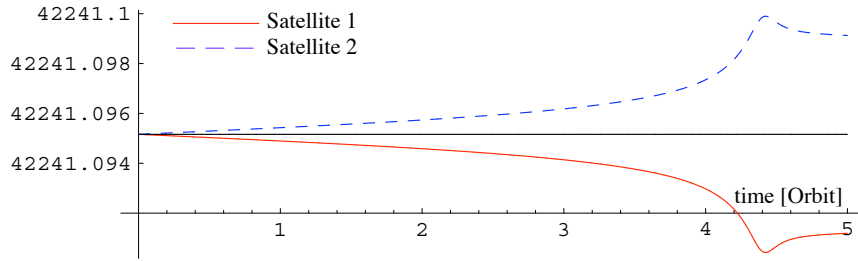
(b) Semi-Major Axes of Both Satellites (km)

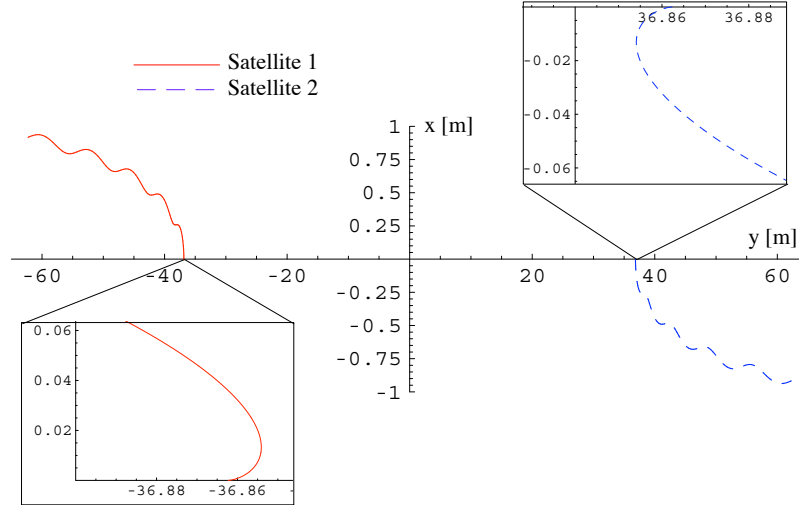**Figure 9: Numerical Simulation with Both Satellites having a +0.1 μC Constant Electric Charge.**

Nonlinear Stabilizing Feedback Control

Using only the Coulomb force between two spacecraft, a nonlinear feedback control law is developed for the spacecraft charge which will stabilize the relative motion between the two craft. Note that no particular relative orbit geometry is enforced at this stage. For unperturbed Keplerian motion, the exact condition for bounded relative motion is that all satellites must have the same semi-major axis a. Let $\boldsymbol{u} = (a_r, a_\theta, a_h)^T$ be a control vector containing the external accelerations imposed on a craft. The vector components are taken in the rotating LVLH frame. Let $\boldsymbol{e}$ be a 6-dimensional vector of orbit elements. These orbit elements are invariants of the unperturbed orbit motion. From Gauss' variational equations, given an external acceleration vector $\boldsymbol{u}$, the orbit element vector $\boldsymbol{e}$ will vary according to[14, 15]

$$\dot{\boldsymbol{e}} = [\mathcal{B}(\boldsymbol{e})]\boldsymbol{u} \tag{13}$$

where $[\mathcal{B}(\boldsymbol{e})]$ is a 6×3 dimensional control influence matrix. Note that this matrix will be time varying and dependent on the true anomaly f. The center LVLH frame is attached to the mass center of the CSF. Since the Coulomb forces are internal forces of the CSF, the mass center motion will be unaffected by these Coulomb forces. Let $\boldsymbol{e}$ be the orbit elements of the center motion, while $\boldsymbol{\epsilon}$ is a M-dimensional subset of $\boldsymbol{e}$ containing the orbit elements that are to be controlled. Because the

(a) Relative Orbit Motion As Seen by Mean LVLH Frame
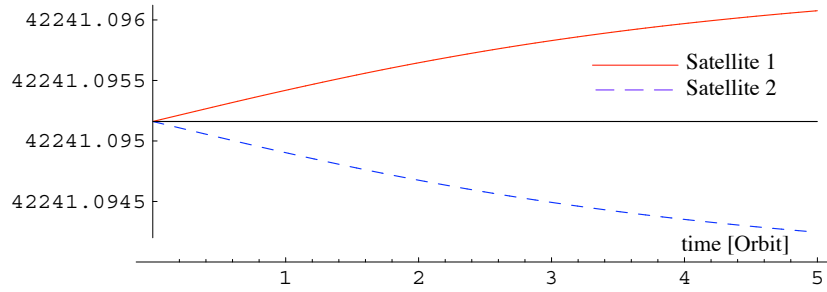
(b) Semi-Major Axes of Both Satellites (km)

Figure 10: Numerical Simulation with a Satellite 1 having +0.1 μC and Satellite 2 having a -0.1 μC Constant Electric Charge.

CSF dimensions are no larger than a few hundred meters in size, we can approximate $e \approx e_1 \approx e_2$ and express the differential equations for ϵ_i through

$$\dot{\boldsymbol{\epsilon}}_1 \approx [B(\boldsymbol{e})]\boldsymbol{u}_1 \tag{14a}$$

$$\dot{\boldsymbol{\epsilon}}_2 \approx [B(\boldsymbol{e})]\boldsymbol{u}_2 \tag{14b}$$

where the $M \times 3$ dimensional matrix $[B(\boldsymbol{e})]$ is a submatrix of $[\mathcal{B}(\boldsymbol{e})]$. To simplify notation from here on, the matrix $[B(\boldsymbol{e})]$ is referred to as $[B]$ and the dependency on $\boldsymbol{e}$ is implied.

The desired set of orbit element differences are expressed through the vector $\Delta\boldsymbol{\epsilon}$. To achieve bounded relative motion, for example, we would set $\Delta a = 0$. The tracking error $\delta\boldsymbol{\epsilon}$ between the spacecraft 1 and 2 orbit elements and the desired orbit element difference is expressed as

$$\delta\boldsymbol{\epsilon} = \boldsymbol{\epsilon}_1 - \boldsymbol{\epsilon}_2 - \Delta\boldsymbol{\epsilon} \tag{15}$$

Because the desired orbit element difference vector is constant and $\Delta\dot{\boldsymbol{\epsilon}} = 0$, the differential equation of the orbit element tracking error vector is

$$\delta\dot{\boldsymbol{\epsilon}} = \dot{\boldsymbol{\epsilon}}_1 - \dot{\boldsymbol{\epsilon}}_2 = [B](\boldsymbol{u}_1 - \boldsymbol{u}_2) \tag{16}$$

Due to the Coulomb forces being internal forces of the CSF, Newton's third law specifies that these two spacecraft forces must be equal in magnitude and opposite in direction. Assuming both spacecraft have the same mass m, the control acceleration vector $\boldsymbol{u}$ satisfies

$$\boldsymbol{u} = \boldsymbol{u}_1 = -\boldsymbol{u}_2 \tag{17}$$

The tracking error differential equation in Eq. (16) is now expressed as

$$\delta\dot{\boldsymbol{\epsilon}} = 2[B]\boldsymbol{u} \tag{18}$$

Let the orbit element error based feedback law be defined as

$$\boldsymbol{u} = -[B]^T[K]\delta\boldsymbol{\epsilon} \tag{19}$$

where the $M \times M$ dimensional gain matrix $[K]$ is symmetric positive definite. To prove stability of this control, the positive definite, radially unbounded Lyapunov function $V(\delta\boldsymbol{\epsilon})$ is introduced:

$$V(\delta\boldsymbol{\epsilon}) = \frac{1}{4}\delta\boldsymbol{\epsilon}^T[K]\delta\boldsymbol{\epsilon} \tag{20}$$

The Lyapunov rate $\dot{V}$ is found to be

$$\dot{V} = \frac{1}{2}\delta\boldsymbol{\epsilon}^T[K]\delta\dot{\boldsymbol{\epsilon}} = \delta\boldsymbol{\epsilon}^T[K][B]\boldsymbol{u} = -\delta\boldsymbol{\epsilon}^T[K][B][B]^T[K]\delta\boldsymbol{\epsilon} \leq 0 \tag{21}$$

Since $\dot{V}$ is negative semi-definite, this control is globally stabilizing, but not necessarily asymptotically stabilizing. This type of orbit element based feedback control has been used previously in References 15–18 to control both inertial and relative orbits. If the complete control acceleration vector $\boldsymbol{u}$ is realizable, then it has been shown in these references that this control is also asymptotically stabilizing. Being based on orbit elements, this control is valid for circular and elliptic orbits.

However, with the inter-spacecraft Coulomb force it is not possible to generate arbitrary in-plane forces. Let $\tilde{u}$ be the projection of the desired control vector $\boldsymbol{u}$ onto the unit relative position vector $\hat{\boldsymbol{r}}_{21} = \boldsymbol{r}_{21}/r_{21}$. Assuming again that $m_1 = m_2 = m$, we find

$$\tilde{u} = \boldsymbol{u} \cdot \hat{\boldsymbol{r}}_{21} = \boldsymbol{u}^T\hat{\boldsymbol{r}}_{21} = -\delta\boldsymbol{\epsilon}^T[K][B]\hat{\boldsymbol{r}}_{21} \tag{22}$$

If $\tilde{u} \geq 0$, then the control $\boldsymbol{u}$ is attempting to push the spacecraft apart and $q_1 q_2$ should be positive (both craft have same sign charge). If $\tilde{u} < 0$, then the craft should be pulled together and the two craft need to have charges with the opposite sign. Thus, the spacecraft control charges are determined through

$$q_1 = r_{21}\sqrt{\frac{m}{k_c}|\tilde{u}|} \tag{23a}$$

$$q_2 = \begin{cases} +q_1 & \tilde{u} \geq 0 \\ -q_1 & \tilde{u} < 0 \end{cases} \tag{23b}$$

With this charging control law, q_1 will always be positive and q_2 can assume either charge sign. Note that a continuous charging control law is assumed here. This assumption is justified since the time to reach a maximum spacecraft charge is on the order of milli-seconds,[5] while the continuous control

variations are on the order of orbit periods (several hours). Thus, for all practical purposes, we can assume here that the desired spacecraft charge will be achieved instantaneously. The spacecraft 1 and 2 charges will cause craft 1 to have a true acceleration $\boldsymbol{\alpha}_1$ of

$$\boldsymbol{\alpha}_1 = \frac{k_c}{m} \frac{r_{21}^2 \left(\frac{m}{k_c} \tilde{u} \right)}{r_{21}^2} \hat{\boldsymbol{r}}_{21} = \tilde{u} \hat{\boldsymbol{r}}_{21} \tag{24}$$

Again, note that $\boldsymbol{\alpha} = \boldsymbol{\alpha}_1 = -\boldsymbol{\alpha}_2$ if both spacecraft have equal mass. Since $\boldsymbol{\alpha}$ is the true acceleration vector being applied to spacecraft 1 (versus the ideal control acceleration $\boldsymbol{u}$), the differential equation for the tracking error vector $\delta\boldsymbol{\epsilon}$ becomes

$$\delta\dot{\boldsymbol{\epsilon}}_1 = 2[B]\boldsymbol{\alpha} \tag{25}$$

where the vector components of $\boldsymbol{\alpha}$ have implicitly been taken in the rotating center LVLH frame. Substituting this expression into the Lyapunov rate expression in Eq. (21), we find

$$\begin{aligned}
\dot{V} &= \frac{1}{2} \delta\boldsymbol{\epsilon}^T [K] \delta\dot{\boldsymbol{\epsilon}} = \delta\boldsymbol{\epsilon}^T [K][B]\boldsymbol{\alpha} \\
&= \delta\boldsymbol{\epsilon}^T [K][B] \hat{\boldsymbol{r}}_{21} \tilde{u} \\
&= \delta\boldsymbol{\epsilon}^T [K][B] \hat{\boldsymbol{r}}_{21} (\boldsymbol{u}^T \hat{\boldsymbol{r}}_{21}) \\
&= \delta\boldsymbol{\epsilon}^T [K][B] \hat{\boldsymbol{r}}_{21} (-\delta\boldsymbol{\epsilon}^T [K][B] \hat{\boldsymbol{r}}_{21}) \\
&= -\left(\hat{\boldsymbol{r}}_{21}^T [B]^T [K] \delta\boldsymbol{\epsilon} \right)^2 \leq 0
\end{aligned} \tag{26}$$

Since $\dot{V}$ is negative semi-definite, the spacecraft charging control law will be globally stabilizing, while asymptotic stability is not guaranteed at this point. In practice, however, global stability is not provided since the Debye length limits the effectiveness of the Coulomb forces. While it has been shown in References 15–18 that the vector $[B]^T [K] \delta\boldsymbol{\epsilon}$ cannot be zero for all time unless $\delta\boldsymbol{\epsilon}$ is zero, the scalar term $\hat{\boldsymbol{r}}_{21}^T [B]^T [K] \delta\boldsymbol{\epsilon}$ can easily be zero for a non-zero tracking error $\delta\boldsymbol{\epsilon}$. For example, assume that the satellites have no out-of-plane relative motion (relative to center LVLH frame). If a non-zero inclination angle difference is desired to achieve out-of-plane relative motion, it is impossible that the spacecraft Coulomb forces could achieve this, because they are only able to produce in-plane accelerations. Further, if multiple orbit elements are to be controlled with this charging control law, then the controls required to reduce the various tracking errors will compete against each other and it is simple to reach a local minima where $\dot{V}$ is zero for a non-zero $\delta\boldsymbol{\epsilon}$. Thus, this general charging control law does guarantee Lyapunov stability, but not convergence.

Next, let us investigate what occurs, stability wise, if the charges are only allowed to reach an upper limit of q_{max}. If charge saturation occurs, then the spacecraft charges are determined through

$$q_1 = q_{\text{max}} \tag{27}$$

$$q_2 = \begin{cases} +q_{\text{max}} & \tilde{u} \geq 0 \\ -q_{\text{max}} & \tilde{u} < 0 \end{cases} \tag{28}$$

Because $q_1 q_2 = q_{\text{max}}^2 \text{sgn}(\tilde{u})$ during saturation, the acceleration of spacecraft 1 due to this limited charge is then given by

$$\boldsymbol{\alpha}_1 = -\boldsymbol{\alpha}_2 = \boldsymbol{\alpha} = \frac{k_c}{m} \frac{q_{\text{max}}^2}{r_{21}^2} \hat{\boldsymbol{r}}_{21} \text{sgn}(\tilde{u}) \tag{29}$$

The Lyapunov rate of Eq. (21) is now expressed as

$$\dot{V} = \delta\boldsymbol{\epsilon}^T[K]\delta\dot{\boldsymbol{\epsilon}}^T = \delta\boldsymbol{\epsilon}^T[K][B]\frac{k_c}{m}\frac{q_{\max}^2}{r_{21}^2}\hat{\boldsymbol{r}}_{21}\text{sgn}(\tilde{u})$$

$$= \frac{k_c}{m}\frac{q_{\max}^2}{r_{21}^2}\delta\boldsymbol{\epsilon}^T[K][B]\hat{\boldsymbol{r}}_{21}\text{sgn}\left(-\delta\boldsymbol{\epsilon}^T[K][B]\hat{\boldsymbol{r}}_{21}\right) \tag{30}$$

$$= -\frac{k_c}{m}\frac{q_{\max}^2}{r_{21}^2}\left|\hat{\boldsymbol{r}}_{21}^T[B]^T[K]\delta\boldsymbol{\epsilon}\right| \leq 0$$

Since $\dot{V}$ is negative semi-definite, we are guaranteed global stability of this saturated control law. However, due to the limited effectiveness of the Coulomb force due to the Debye length, in practice this saturated control will have a limited domain of stability. Further, since the scalar term $\hat{\boldsymbol{r}}_{21}^T[B]^T[K]\delta\boldsymbol{\epsilon}$ can be zero for non-zero tracking error $\delta\boldsymbol{\epsilon}$, this saturated charging control cannot guarantee asymptotic convergence.

Let us examine the convergence of a special case of this charging control law. Assume that the only goal is to achieve bounded relative motion. This requires that $\Delta\boldsymbol{\epsilon} = (\Delta a) = 0$. The control influence matrix $[B]$ for the semi-major axis is given by[14, 15]

$$\dot{a} = \frac{2a^2}{h}\left[e\sin f \quad \frac{p}{r} \quad 0\right]\boldsymbol{u} = [B]\boldsymbol{u} \tag{31}$$

where h is the orbit momentum magnitude, p is the semilatus rectum, and r is the current center LVLH frame orbit radius. For this case the control vector $\boldsymbol{u}$ simplifies to

$$\boldsymbol{u} = -[B]^T K\delta a \tag{32}$$

with the gain $K > 0$ being a scalar parameter. The Lyapunov rate expression in Eq. (30) is reduced to

$$\dot{V} = -\delta a^2 K^2([B]\hat{\boldsymbol{r}}_{21})^2 \leq 0 \tag{33}$$

To prove that the semi-major axis tracking error δa will asymptotically go to zero, we need to show that the scalar term $[B]\hat{\boldsymbol{r}}_{21}$ cannot remain zero. Defining $\hat{\boldsymbol{r}}_{21} = (\rho_1, \rho_2, \rho_3)^T/r_{21}$, the term $[B]\hat{\boldsymbol{r}}_{21}$ is expressed as

$$[B]\hat{\boldsymbol{r}}_{21} = \frac{2a^2}{hr_{21}}\left(\rho_1 e\sin f + \rho_2\frac{p}{r}\right) \tag{34}$$

Assuming a near-circular nominal CSF orbit (which is common for most GEO applications), the above condition can be simplified to

$$[B]\hat{\boldsymbol{r}}_{21} = \frac{2a^2}{hr_{21}}\rho_2 \tag{35}$$

This means that we need to demonstrate that ρ_2 cannot be zero for all time if δa is non-zero. The relative orbit coordinate $\rho_2(f)$ can be approximated as[19]

$$\rho_2(f) = a(\delta\omega + \delta M(f) + \cos i\ \delta\Omega) + 2a\sin f\ \delta e \tag{36}$$

The linearized mean anomaly drift $\delta M(f)$ is expressed as[20]

$$\delta M(f) = \delta M_0 - \frac{3}{2} f \frac{\delta a}{a} \tag{37}$$

Using Eqs. (36) and (37), the term $[B]\hat{\boldsymbol{r}}_{21}$ can be written as

$$[B]\hat{\boldsymbol{r}}_{21} = \frac{2a^2}{h r_{21}} \left(\delta\omega + \delta M_0 + \cos i\, \delta\Omega - \frac{3}{2} f \frac{\delta a}{a} + 2a \sin f\, \delta e \right) \tag{38}$$

For Eq. (38) to be zero for all time, the static term $(\delta\omega + \delta M_0 + \cos i\, \delta\Omega)$, the secular term $\left(-\frac{3}{2} f \frac{\delta a}{a}\right)$, and the trigonometric term $(2a \sin f\, \delta e)$ must vanish independently. This leads to the conditions that $\delta\omega + \delta M_0 + \cos i\, \delta\Omega = 0$, $\delta a = 0$, and $\delta e = 0$ for $[B]\hat{\boldsymbol{r}}_{21}$ to be zero for all time. Thus, since $[B]\hat{\boldsymbol{r}}_{21}$ cannot remain zero for a non-zero δa, the semi-major axis control in Eq. (32) is indeed asymptotically stabilizing in δa.

For the saturated version of the semi-major axis Coulomb control, the Lyapunov rate expression in Eq. (30) reduces to

$$\dot{V} = -\frac{k_c}{m} \frac{q_{\max}^2}{r_{21}^2} K |\delta a|\, |[B]\hat{\boldsymbol{r}}_{21}| \tag{39}$$

Since $[B]\hat{\boldsymbol{r}}_{21}$ cannot remain zero for non-zero δa, the saturated version of this control is also asymptotically stabilizing.

Numerical Simulation of Stabilizing Control

The performance of the spacecraft charging control law in Eq. (23) is illustrated through a numerical simulation. For satellite 1, the simulation setup of the static charge simulation is repeated here with the inertial nonlinear equations of motion in Eq. (12) being numerically solved. The satellite 2 orbit elements are equal to those of satellite 1 except for the semi-major axis, which is 20 meters larger, and the eccentricity, which is 0.000001. If left uncontrolled, the two satellites would drift apart at about 190 meters per orbit. Let the vector of controlled orbit elements be

$$\boldsymbol{\epsilon} = \begin{pmatrix} a \\ \omega + M_0 \end{pmatrix} \tag{40}$$

The desired orbit element differences are given by

$$\Delta\boldsymbol{\epsilon} = \begin{pmatrix} 0 \text{ km} \\ 0^{\text{o}} \end{pmatrix} \tag{41}$$

This will attempt to establish a bounded relative motion (i.e. cancel the difference in semi-major axes) and avoid having the point about which each satellite is orbiting (as seen by the center LVLH frame) wander from the center LVLH frame origin. For this particular set of elements, the matrix $[B]$ is given by[14]

$$[B] = \begin{bmatrix} \frac{2a^2}{h} e \sin f & \frac{2a^2}{h} \frac{p}{r} & 0 \\ -\frac{ae}{h(a+b)} p \cos f - \frac{2br}{ah} & \frac{(p+r)\sin f ae}{h(a+b)} & -\frac{r \sin\theta \cos i}{h \sin i} \end{bmatrix} \tag{42}$$
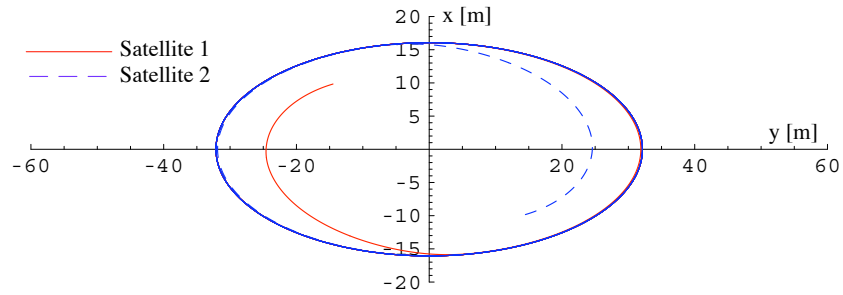
Note that because this simulation setup involves exclusively in-plane relative motion, only in-plane motion will result with the Coulomb control. The nonlinear Cartesian equations of motion in
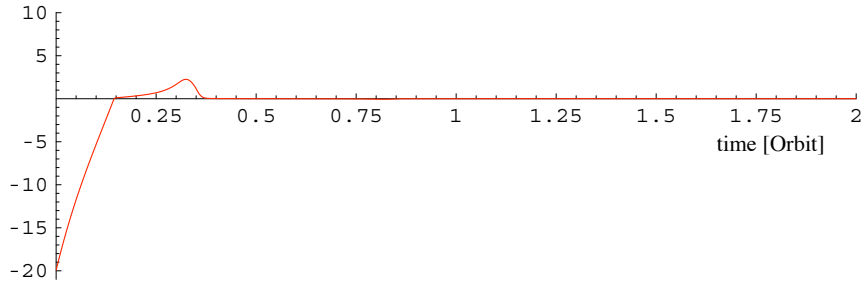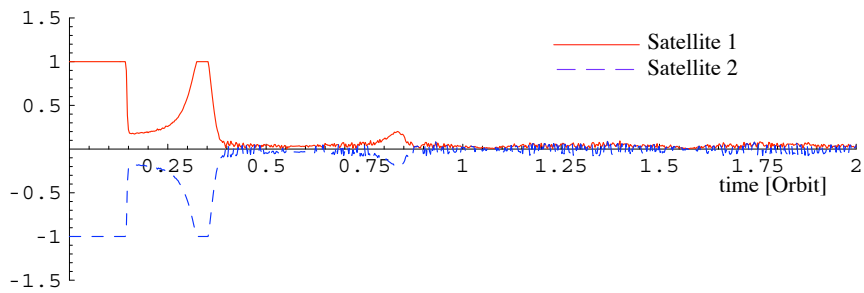
(a) Semi-Major Axis Tracking Error δa (m)
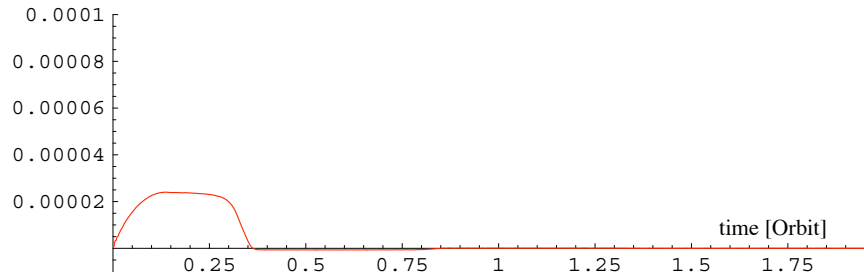
(b) Tracking Error $\delta\omega + \delta M$ (deg)

(c) Relative Orbits As Seen by Center LVLH Frame

(d) Satellite Charges (μC)

Figure 11: Numerical Simulation with the Coulomb Charge Controlling both δa and $\delta\omega + \delta M_0$ Tracking Errors.

Eq. (12) are solved in the numerical simulation. The spacecraft charge is limited to $q_{max} = 1\mu C$. The gain matrix used is $[K] = \text{diag}(5 \cdot 10^{-12}, a \cdot 10^{-8})$. The simulation results are illustrated in Figure 11. With the chosen gains and this particular set of initial orbit element errors, the tracking errors are reduced to near zero within less than 0.5 orbits. Note, however, that the closed-loop dynamics were found to be sufficiently nonlinear to make it very sensitive to the chosen control gains. While the current simulation shows nearly no overshoot in the tracking error dynamics, if other initial tracking errors are used with the same gains then the control might take several orbits to converge. In these cases the semi-major axis typically still converged within an orbit or two to the desired values, but the initial latitude angle $\omega + M_0$ took many more orbits periods to converge. For all numerical simulations runs performed with this particular ϵ vector in Eq. (40), the tracking errors always appeared to converge to zero. However, no analytical proof of asymptotic convergence of this $\Delta\epsilon$ is provided in this paper. If other elements such as the eccentricity or the inclination angle were controlled (the later only with initial out-of-plane relative motion present), then these particular orbit elements only approached the desired values for particular sets of gains and initial tracking errors. As was discussed in the control analysis, for general sets of controlled orbit elements we are only guaranteed stability and not asymptotic convergence.

The charges required by either spacecraft are shown in Figure 11(d). As the control theory predicted, despite charge saturation occurring, the control is still able to stabilize the tracking errors. The small chatter like behavior shown near zero charge is due to numerical limitations. Since the simulation is performed in inertial Cartesian space and the relative motion is very small, small differences of large numbers are computed. Even using double precision variables, the standard nonlinear mapping between Cartesian coordinates and orbit elements results in some numerical degradation. A simulation setup in the rotating LVLH frame would avoid this issue. However, performing the simulation in another coordinate space than the one used for the control development allowed for various checks to be performed that the simulation and theory were working properly.

The presented nonlinear feedback law illustrates that it is possible to use the Coulomb force to bound and control the relative motion of a dynamic two-satellite formation of equal mass. Future research will look into extending this control theory to satellites of different mass and to CSFs containing more than two satellites. Of particular interest is also applying impulsive feedback laws to the CSF control problem. With the presented continuous control, convergence of tracking errors is often hampered by competing control goals with limited feasible acceleration vectors. With the large bandwidth of the Coulomb charging process, it should be possible to implement an impulsive control scheme that would selectively correct particular elements without influencing others. Further, the use of optimal control techniques looks promising to establish efficient tracking for arbitrary tracking errors.

Conclusion

Spacecraft formation flying control using Coulomb Forces in Earth orbit is only viable in high-altitude (HEO-GEO) due the electrical shielding properties of the space plasma. The benefits of exploiting inter-spacecraft Coulomb forces are a virtually propellantless method to perform relative orbit corrections with the capability of operating at very high bandwidths. For small spacecraft separation distances of the order of tens of meters, the magnitude of the Coulomb force is as good or better than many high efficiency ion propulsion methods at a fraction of the power requirement. Static equilibrium conditions have been found that allow the satellites to remain in fixed positions relative to each other. These static crystal-like formations are impossible with conventional satellite formations where the crafts tend to orbit about each other. The control challenges of such static for-

mations are discussed. Further, the dynamic motion and control of a two-satellite CSF is explored. A nonlinear control is presented which is able to bound the relative motion between two close satellites by asymptotically equalizing the two satellite semi-major axes. The continuous charging feedback control can also be used to control general orbit element difference with guaranteed stability, but not necessarily asymptotic convergence. These early results illustrate the exciting potential of CSF, while outlining many dynamic and control challenges that need to be solved to make this tight formation flying control concept a viable solution.

References

[1] MULLEN, E. G., GUSSENHOVEN, M. S., and HARDY, D. A, "SCATHA Survey of High-Voltage Spacecraft Charging in Sunlight", *Journal of the Geophysical Sciences*, Vol. 91, 1986, pp. 1074–1090.

[2] GARRETT, H. B., SCHWANK, D. C., and DEFROST, S. E., "A Statistical Analysis of the Low Energy Geosynchronous Plasma Environment. -I Protons", *Planetary Space Science*, Vol. 29, 1981b, pp. 1045–1060.

[3] GARRETT, H. B., SCHWANK, D. C., and DEFROST, S. E., "A Statistical Analysis of the Low Energy Geosynchronous Plasma Environment. -I Electrons", *Planetary Space Science*, Vol. 29, 1981a, pp. 1021–1044.

[4] GARRETT, H. B. and DEFROST, S. E., "An Analytical Simulation of the Geosynchronous Plasma Environment", *Planetary Space Science*, Vol. 27, 1979, pp. 1101–1109.

[5] KING, LYON B., PARKER, GORDON G., DESHMUKH, SATWIK, ET AL., "Spacecraft Formation-Flying using Inter-Vehicle Coulomb Forces", Tech. rep., NASA/NIAC, January 2002, available online at http://www.niac.usra.edu under "Funded Studies.".

[6] KING, LYON B., PARKER, GORDON G., DESHMUKH, SATWIK, ET AL., "Study of Interspacecraft Coulomb Forces and Implications for Formation Flying", *AIAA Journal of Propulsion and Power*, Vol. 19, No. 3, May–June 2003, pp. 497–505.

[7] KONG, E., MILLER, DAVID W., and SEDWICK, R. J., "Exploiting Orbital Dynamics for Aperture Synthesis using Distributed Satellite Systems", *Proceedings of the Space Flight Mechanics Meeting*, Breckenridge, CO, Feb. 7–10 1999, (pp. 385–301), Paper AAS-99-112.

[8] *Interactive Spacecraft Charging Handbook*, Space Environment Effect Program, NASA Marshall Space Flight Center.

[9] NICHOLSON, DWIGHT R., *Introduction to Plasma Theory*, Krieger, 1992.

[10] GOMBOSI, TAMAS I., *Physics of the Space Environment*, Cambridge University Press, 1998.

[11] MARCUCCIA, S., GENOVESE, A., and ANDRENUCCI, M., "Experimental Performance of Field Emission Microthrusters", *Journal of Propulsion and Power*, Vol. 14, No. 5, Sept.–Oct. 1998, pp. 775–781.

[12] GULCZINSKI, FRANK S., DULLIGAN, MICHAEL J., LAKE, JAMES P., ET AL., "Micropropulsion research at AFRL", *AIAA/ASMA/SAE/ASEE Joint Propulsion Conference and Exhibit*, Huntsville, AL, July 16–19 2000, Paper No. 2000-3255.

[13] CHONG, JER-HONG, *Dynamic Behavior of Spacecraft Formation Flying using Coulomb Forces*, Master's thesis, Michigan Technological University, May 2002.

[14] BATTIN, RICHARD H., *An Introduction to the Mathematics and Methods of Astrodynamics*, AIAA Education Series, New York, 1987.

[15] SCHAUB, HANSPETER and JUNKINS, JOHN L., *Analytical Mechanics of Space Systems*, AIAA Education Series, Reston, VA, 2003.

[16] ILGEN, MARC R., "Low Thrust OTV Guidance using Lyapunov Optimal Feedback Control Techniques", AAS/AIAA Astrodynamics Specialist Conference, Victoria, B.C., Canada, Aug. 16–19 1993, Paper No. AAS 93-680.

[17] NAASZ, BO J., *Classical Element Feedback Control for Spacecraft Orbital Maneuvers*, Master's thesis, Virginia Polytechnic Institute and State University, Blacksburg, VA, May 2002.

[18] NAASZ, BO J., KARLGAARD, CHRISTOPHER D., and HALL, CHRISTOPHER D., "Application of Several Control Techniques for the Ionospheric Observation Nanosatellite Formation", AAS/AIAA Space Flight Mechanics Meeting, San Antonio, TX, Jan. 2002, Paper No. AAS 02-188.

[19] SCHAUB, HANSPETER, "Spacecraft Relative Orbit Geometry Description Through Orbit Element Differences", *14th U.S. National Congress of Theoretical and Applied Mechanics*, Blacksburg, VA, June 2002.

[20] SCHAUB, HANSPETER, "Incorporating Secular Drifts into the Orbit Element Difference Description of Relative Orbits", *AAS/AIAA Space Flight Mechanics Meeting*, Ponce, Puerto Rico, February 2003, paper No. AAS 03-115.